2D BUILDING CHANGE DETECTION FROM HIGH RESOLUTION AERIAL IMAGES AND CORRELATION DIGITAL SURFACE MODELS

Nicolas Champion

MATIS Laboratory, Institut Géographique National
2, Avenue Pasteur. 94165 SAINT-MANDE Cedex - FRANCE
Firstname.Lastname@ign.fr

Commission IV/3

KEY WORDS: Change Detection, Buildings, 2D topographic database, DSM, DTM, Updating

ABSTRACT:

Updating 2D databases has become a crucial issue in most mapping agencies. Such a work traditionally starts out with a change detection phase. A subsequent update phase is then carried out to register changes in the up-to-date database. The first phase is by far the most costly and plodding, as it has until now required field or visual inspection (of orthophotos). The main goal of this paper is to present a new method for detecting changes in the building layer of a 2D cadastral database. This method aims at giving potential changes to a human operator for subsequent validation and update registration. In this paper, we propose a new workflow for the change detection process, by splitting it into 2 separate steps. The first step consists in verifying automatically buildings through a hypothesize-and-verify process: the initial description of the database is used to guide the change detection process. The second step consists in extracting new buildings from geometric considerations. In this paper, the method is tested and assessed in a densely built-up area. A specific methodology is firstly employed to estimate the best parameters to use in the system and also to characterise its performance. Results are secondly assessed and show the high potential of our system in such a context.

1 INTRODUCTION

In the past few years, most 2D topographic databases have been completed in developed countries. Most efforts in mapping agencies are now dedicated to the revision / update of such databases. Such a task is particularly time-consuming and tedious, as it is generally carried out manually, by visual inspection of an orthophoto to detect objects to be revised. Therefore, such a work is highly costly: (Steinnocher and Kressler, 2006) estimates that it can cost up to 40% of the whole cost entailed when generating the topographic database from scratch. Semi-automatic procedures also need to be developed. Such procedures are commonly split into 2 steps: in a first change detection step, input data (high resolution aerial or satellite images, laser scanning . . .) are given to an algorithm that then determines focalisation areas where a possible change has taken place; in a second update step, these focalisation areas are given to a human operator for validation and registration. Among all the objects contained in a topographic database, we will focus here on buildings, which play a crucial role in an increasing number of applications, especially in the production of 3D City models (Taillandier, 2005). As shown in Figure 1, a building change can be of several types: destroyed buildings as well as new buildings are obviously changes. Moreover, the modification or the deletion of a part of a building (caused either by a human activity or planimetric inaccuracies in the initial geospatial database) is a change and must be detected by the algorithm.

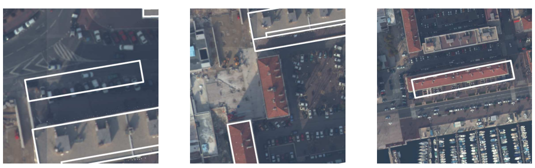

(1) **(2)** **(3)**

Figure 1: Update Problems. **(1) :** Destroyed buildings. **(2) :** New buildings. **(3) :** Planimetric inaccuracies.

1.1 Related works

Since the advent of high-quality digital aerial images and laser scanning, many researches have been carried out to detect changes in the building layer of a 2D digital database.
In Germany, the WIPKA project[1] has been launched to automatically verify a topographic database. Within this scope, a knowledge-driven approach (Busch et al., 2004) is proposed to verify area objects (settlement, industrial areas, cropland . . .) contained in the database: hints are collected from images for each object to be verified (top-down phase) and used to accept or reject the object (bottom-up phase). This study is all the more interesting as it shows that a change detection process is always data-dependent: the specifications of the database to be checked need to be taken into account before building the system design.
In (Steinnocher and Kressler, 2006), an object-based classification is implemented to support the update of existing land use databases. Orthophotos are firstly segmented and each object is classified into 4 classes (identical, plausible, questionable, new) by means of so-called evaluation matrices. Results are promising but show the difficulty to deal with objects assigned to a given class for legal and not physical reasons, typically administrative sections. (Matikainen et al., 2004) proposes a similar object-oriented classification based on laser scanning and digital aerial images but focus on the building theme only. Results are all the best as buildings are big.
(Olsen and Knudsen, 2005) proposes a hierarchical method: a coarse building mask is firstly computed from initial DSM and NIR images, and then refined with respect to object size and form. Eventually, it is compared to the database to update. The authors outline the necessity to compute a DTM from the DSM, as height features are very useful when detecting buildings.
Eventually, other methods exist in literature and could be used in a change detection process, even if they are not originally built for that purpose. For example, the method described in

[1] http://www.ipi.uni-hannover.de/html/forschung/laufend/wipka/wipka.htm, Last Visited: 2007-3-31

Figure 2: Semantic differences: one building can be split into 2 or more objects in the database.

(Rottensteiner et al., 2005) deals with building detection from aerial images and laser scanning. It is based on a hierarchical Dempster-Shafer classification. This method is being adapted to enter the framework of a new EuroSDR Building Change Detection project.

1.2 General Scheme

The main goal of this paper is to present a new method for change detection in the building layer of a 2D geospatial database from digital aerial images. Digital aerial images are chosen as primary input data, as they are most of time necessary for photogrammetric projects and therefore do not imply additional costs, contrary to other data like laser scanning. In our study, only significant changes (with a size larger than 25 m^2) corresponding to new, old, partially destroyed and enlarged buildings are considered. Other inconsistencies (typically, inaccuracies in planimetry) are considered as well.
In Section 2, input data are firstly described. In Section 3, our method is detailed. Section 4 is devoted to the presentation of the results and their evaluation. Eventually, forthcoming research axes are given in concluding remarks.

2 STUDY AREA AND INPUT DATA

The study area is located in Marseille, southern France and corresponds to a very dense urban area.

2.1 Input Data

In our study, RGB and IR aerial images are used, with a Ground Sample Distance (GSD) of 20 cm, a forward and a side lap of 60%. A correlation DSM with a GSD of 20 cm is then derived, with the method described in (Pierrot-Deseilligny and Paparoditis, 2006). Moreover, true RGB and IR orthophotos are computed. Eventually, a tree mask and a lawn mask are automatically derived, with the method described in (Iovan et al., 2007).

2.2 The database to update

The database to update is a cadastral map, composed of 3 layers: the building layer is here the object of the revision and is described now. As buildings are captured in the field by surveyors, their boundaries are given in the database by walls and not gutters (like in DSM or orthophotos). Moreover, as they are initially built for tax purposes, the limits of a building actually correspond to the limits of an ownership: when shared by 2 different homeowners, one physical building is systematically split into 2 objects (Figure 2). These 2 particularities have been taken into account when designing the system.

3 METHOD

A new workflow is proposed for this study: contrary to studies found in literature, the change detection process is here split into 2 separate steps. In a first (so-called automatic verification of the database) step, the initial scene description of the database is used to guide the detection of old and geometrically shifted buildings and to validate existing buildings. In a second (so-called detection of new buildings) step, a specific algorithm allows detecting new buildings. Combined together, these 2 steps perform a comprehensive change detection workflow.

3.1 Step I: Automatic Verification of the database

This first step is composed of 3 stages: clues are firstly collected for each object to be checked (1). A similarity measure is then computed (2) to give a final acceptance or rejection decision (3).

3.1.1 Features Extraction Following the recommendations found in (Olsen and Knudsen, 2005), robust geometric criteria are preferred to radiometric criteria, too dependent on illumination conditions, and not necessarily robust to recent buildings that are often built with various, non-conventionnal (and sometimes uncommon) material.
A large amount of geometric criteria can be found in litterature: objects height (Jordan et al., 2002), height textures based on the surface roughness (Rottensteiner et al., 2005), structural (form) features (Müller and Zaum, 2005), edges delimitation (Tarsha-Kurdi et al., 2006) . . . In our *vector* database, objects to be checked are well structured, as they are represented by their boundaries. Therefore, features based on edges (i.e. contours / height discontinuities) appear to be the best adapted.
In our work, contours are extracted in the initial DSM with the classical gradient operator (Deriche, 1987), followed by a hysteresis detection of local maxima in the direction of gradients, with a sub-pixel (0.5 pixel) accuracy. Sub-pixel local maxima are then chained and poligonized to obtained DSM contours.

3.1.2 Similarity Measure

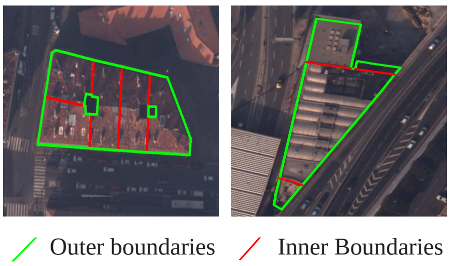

Figure 3: Inner and Outer boundaries.

Selection of pertinent building boundaries As previously mentioned, the building boundaries in the database correspond to limits of ownerships. Therefore, as shown in Figure 3, boundaries are split into 2 categories: inner boundaries and outer boundaries. Inner boundaries (i.e. shared by 2 adjacent buildings) correspond to the intangible limit between 2 ownerships and they only seldom correspond to a physical (height, even radiometric) discontinuity. By contrast, outer boundaries (i.e. belonging to only one building) must have a corresponding height discontinuity in DSM. Moreover, boundaries covered by vegetation are not verifiable. Therefore, only pertinent boundaries (i.e. outer boundaries not covered by vegetation) are kept in the process for subsequent verification.

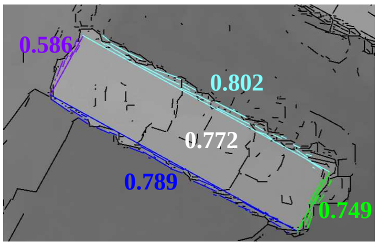

Figure 4: Description of the similarity measure. DSM contours extracted from the Canny-Deriche edge detector are pictured in black over the DSM. Each pertinent boundary is represented with its associated DSM contours and similarity measure. In white, the over-all similarity measure assigned to the building.

Definition of the similarity measure For each building to be checked, pertinent boundaries are selected. Then, as illustrated in Figure 4, for each boundary, DSM contours, located at a given distance from it and fulfilling a preset relative orientation with respect to it, are selected (top-down phase). A first measure is computed per boundary: it is based on the rate of coverage of selected contours on it. At the end, the building is assigned an over-all similarity measure that corresponds to a weighted mean of previous boundary measures.

More formally, let B be a building to be checked and b_j, a pertinent boundary (Refer to Figure 5 for an illustration). A Region Of Interest ROI_j is then defined for each pertinent boundary b_j, as a buffer given by its width d_0, centred on and aligned with b_j. The similarity measure SM is given by:

$$SM = \frac{\sum_{b_j \in B} \|b_j\| \, \rho\left(b_j, \left\{c_i : c_i \in ROI_j \ and \ |\theta_i^j| \leq \theta_0\right\}_i\right)}{\sum_{b_j \in B} \|b_j\|} \quad (1)$$

where:

- c_i is a DSM contour
- θ_i^j is the relative orientation between c_i and b_j
- θ_0 is a preset relative orientation
- $\|\|$ gives the length of b_j
- ρ computes the coverage rate between b_j and selected contours

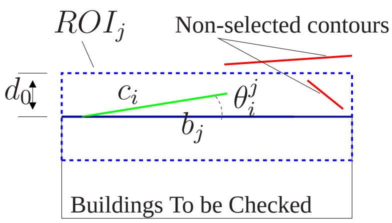

Figure 5: Similarity measure - Sketch.

In our application, d_0 and θ_0 are respectively set to 2m and 10°. Performance tests, similar to the one described in Section 4.1, show that these parameters are not critical.

3.1.3 Decision-making Module Once similarity measures are computed per building, the bottom-up phase is completed by a rule-based acceptance or rejection decision. Objects are here classified into 3 classes:

- "Destroyed" if $SM \leq T_L$
- "Modified" if $SM \geq T_L \ and \ SM \leq T_H$
- "Validated" if $SM \geq T_H$

Objects contained in the 2 first classes are considered changes and are also given to a human operator for validation and update purposes (not described here). Remaining objects are considered unchanged. In our application, T_L is set to 0.1 and T_H is set to 0.61. T_H is by far the most important parameter in our system, as it fully determines "Change" from "No Change" objects. Performance tests are introduced in Section 4.1 and applied to estimate the best value to use.

3.2 Step II: Detection of new buildings

Once the buildings of the database have been verified, new buildings remain to be detected. For that purpose, a new workflow based on the initial DSM and a reliable and automatically computed DTM is proposed.

3.2.1 Automatic Estimation of a DTM As illustrated in Figure 7, a DTM is automatically derived from the initial DSM and the above-ground mask with the algorithm described in (Champion and Boldo, 2006). Note that the above-ground mask is composed of the initial tree mask and a building mask, directly derived from the database to update. Buildings, labelled as destroyed in Step I, are removed from the mask, as they potentially correspond to ground.

The algorithm used in our study belongs to surface-based algorithms: the DTM to reconstuct is supposed to be a regular surface (defined by some internal properties) and is estimated so that it best fits observation data (points out of the above-ground mask). A special attention has been paid to deal with outliers (above-ground points not present in the above-ground mask i.e. cars, street furniture and above all new buildings). As such points systematically deviate the DTM upwards, a module based on the M-estimator theory is integrated to the algorithm to filter them out: once outliers are removed, the final ground surface fits true ground points (inliers) and best reconstructs the true topographic surface, as shown in Figure 6.

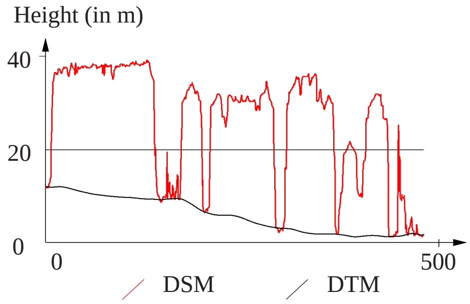

Figure 6: Profile along the red arrow (See Figure 7-1). The DTM calculated with our algorithm perfectly clings to lowest points in streets and courtyards.

3.2.2 Detection of new buildings A normalised DSM (nDSM) is then generated by substracting this DTM from the original DSM. Easy-to-use height thresholding techniques applied to this nDSM leads to the extraction of above-ground objects (in our application, the height threshold is set to 2m). Man-made structures and tree objects already present in the database to update or the tree mask are then filtered out and no significant above-ground objects are subsequently eliminated by morphological opening. Remaining objects correspond to new buildings (Figure 7-6).

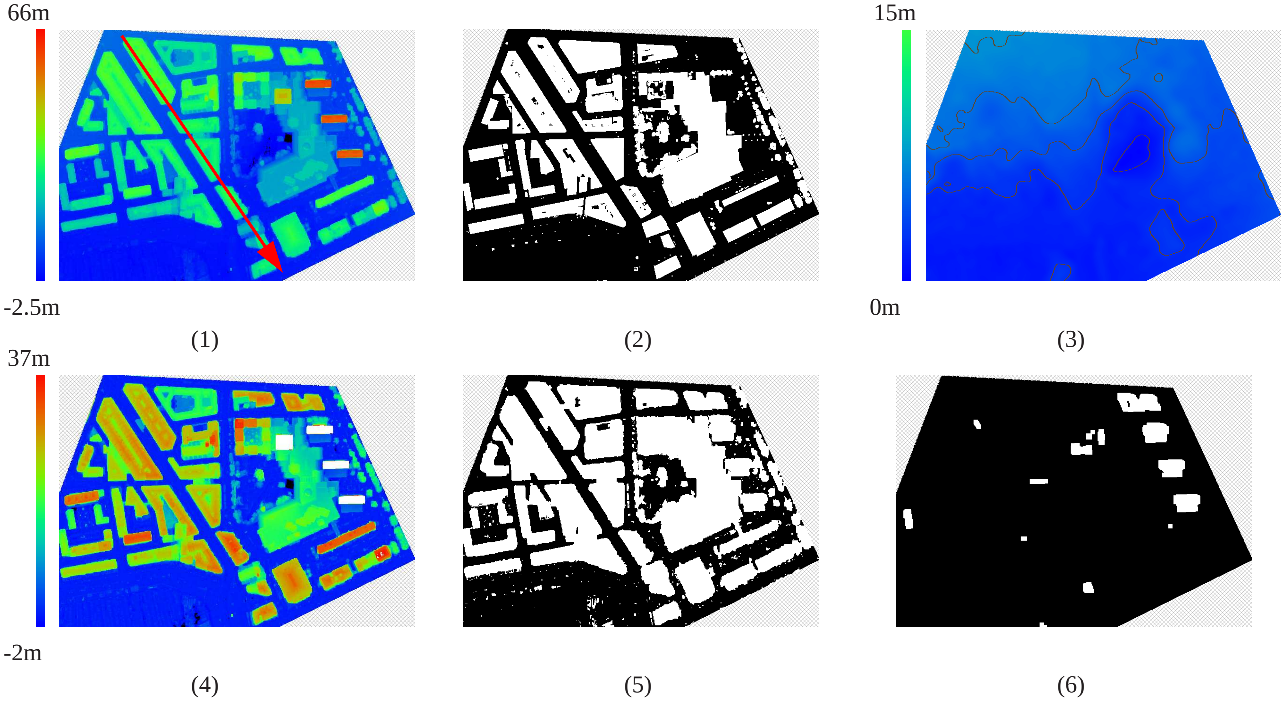

Figure 7: Detection of new buildings in Marseille. **(1) :** Initial DSM. **(2) :** Initial Above-ground Mask. $\{Trees \cup Buildings\} - \{Destroyed\ Buildings\}$ **(3) :** Automatically processed DTM (Contour lines are superimposed over the DTM, with a contour interval of 3m). **(4) :** Building Height. **(5) :** Processed Above-Ground Mask. **(6) :** New building Mask.

4 RESULTS AND EVALUATION

The database to update contains 256 buildings. 238 are still present in the database to update, 11 buildings correspond to modifications or planimetric inaccuracies and 7 buildings have been demolished. Moreover, 9 buildings have been built.
In this section, the methodology chosen to determine the best threshold T_H to use in the decision-making process is firstly described. Results are then given, assessed and discussed.

4.1 ROC Curves: How to optimise and characterise the performance of a system?

The outcome of our process is also a binary classification, in which buildings are labelled either as ”Change” or ”No Change”. When comparing this classification to a reference classification (labels are here edited manually), 4 possible cases happen, as detailed in the 2×2 confusion matrix (Table 1).

True Algo	Change	No Change
Change	TP	FP
No Change	FN	TN

Table 1: Confusion Matrix

(Fawcett, 2004) proposes to evaluate a decision-making process by plotting its Receiver Operating Characteristic aka ROC curve. That comes down to plot the True Positive Rate (TPR) vs. the False Positive Rate (FPR), as the decision threshold is varied, where the TPR and FPR rates are respectively defined as:

$$TPR = \frac{TP}{TP + FN} \in [0; 1] \qquad (2)$$

$$FPR = \frac{FP}{FP + TN} \in [0; 1] \qquad (3)$$

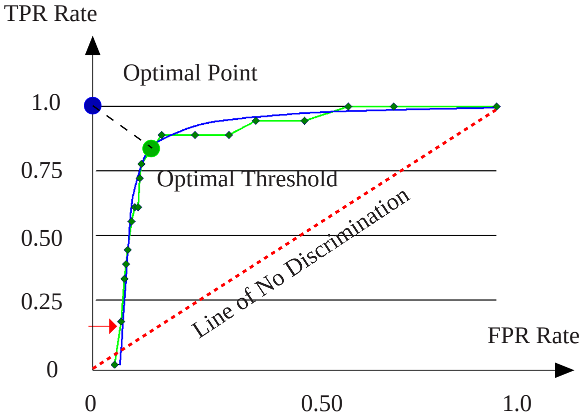

Figure 8: Performance Evaluation. In green, our experimental ROC curve. In blue, its corresponding trend curve.

In ROC curves (Figure 8), the so-called optimal point is located in the upper left corner and corresponds to a perfect classification, in which all changes are detected whitout any FP. Points located in the main diagonal (aka line of no discrimination) correspond to the result of a process that would randomly label buildings. Moreover, a test is said to be non-discriminative if its corresponding point in ROC space is situated below the main diagonal. Conversely, a test is all the more discriminative as its corresponding point is closer to the optimal point: the TP (benefit) / FP (cost) rate is then optimized.
To assess the performance of our system, the T_H threshold is also tuned from 0 to 1 and corresponding TPR and FPR rates are calculated and plotted in ROC space. As shown in Figure 8, the optimal threshold is easily derived and here corresponds to 0.61. Note that a small shift (highlighted with a red arrow) occur at the origin of the curve, which means the FPR rate is never null re-

gardless of the value of T_H. Such a characteristic is caused by both the database and the system design. Indeed, 11 unchanged buildings correspond to small structures in courtyards. All their boudaries are shared with other buildings and also considered inner boundaries in the selection phase (Subsection 3.1): in that case, the similarity measure is not computed; instead, an alert is systematically (and here wongly) sent.

4.2 Change Detection Results

The results of our change detection process is now presented (Figure 9) in a similar way as the so-called Traffic Light Paradigm (Förstner, 1994): destroyed buildings are highlighted in red, modified buildings in yellow and new buildings in orange. Concerning “No Change” objects, they are highlighted in green.

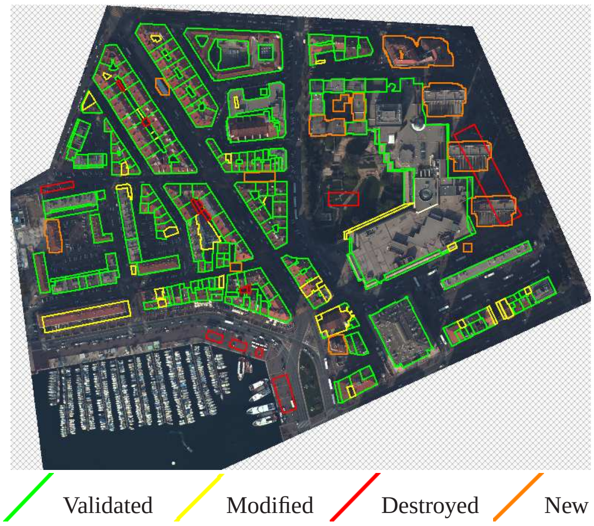

Figure 9: Change Detection Results in Marseille Test Area.

4.3 Evaluation and Discussion

4.3.1 Quality Measures As mentioned in (Rottensteiner et al., 2005), 2 quality measures are classicaly used to assess the results of a change detection process: the completeness and the correctness.

$$Completeness\ (TPR) = \frac{TP}{TP + FN} \in [0;1] \tag{4}$$

$$Correctness = \frac{TP}{TP + FP} \in [0;1] \tag{5}$$

As explained in (Heipke et al., 1997), these 2 measures respectively answer the questions: (1) How complete is the change detection? (2) How correct is the change detection? From a practical point of view, the completeness refers to errors kept in the final database, once updated. As for the correctness, it refers to the time lost by a human operator to check unchanged buildings. As expected in a change detection process, the FN rate must tend towards 0 (i.e. the completeness towards 1) whereas the FP rate must be as small as possible (i.e. the correctness as close to 1 as possible).

4.3.2 Quantitative Results The results of the evaluation are depicted in Figure 10 and also given in the confusion matrix (Table 2).

4.4 Discussion

As shown in Figure 11, the 2 non-detected changes (1) correspond to minor changes: the courtyard is not properly located in

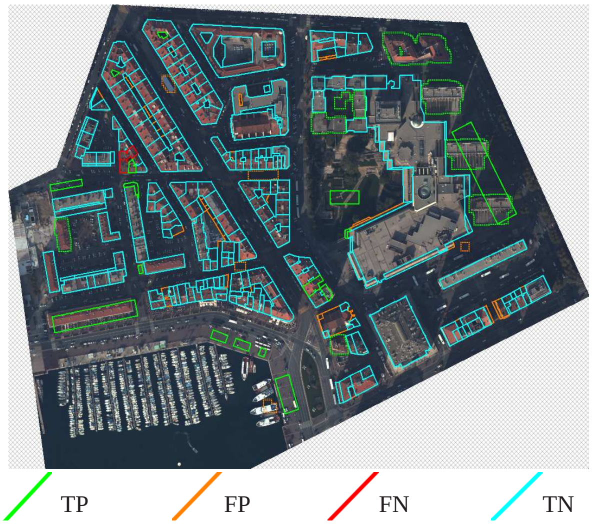

Figure 10: Evaluation in Marseille Test Area.

Algo \ True	Change	No Change
Change	25 [9.3%]	45[16.7%]
No Change	2 [$\leq$ 1%]	197 [73.2%]
Completeness = 0.93		
Correctness = 0.37		

Table 2: Confusion Matrix and Quality Measures

planimetry but validated.
Concerning false alarms (False Positive), they are of several types: they can correpond to the previously mentioned small structures in courtyards (2) or building-like structures, such as prefabs (3) or footbridges. Moreover, lots of false alarms correspond to inaccuracies / false correlation in the initial DSM. For example, the height of narrowest streets in shadows areas is sometimes overestimated and, at the end, considered new buildings by the algorithm (4). Nevertheless, this relatively high FP rate (approximately twice the number of factual changes) has to be put into perspective.
At first sight, this relatively high FP rate may appear to be a high limitation of our system. On one hand, it prevents us to consider a fully automatic change detection process. On the other hand, it systematically leads a human operator to check uselessly unchanged buildings. Nevertheless, the matter-of-fact / pragmatic approach employed in this study (that consists in splitting the change detection problem into 2 easier subtasks) allows checking only one quarter of the database (70/256 buildings) with very satisfying results: only 2 minor changes are not detected; moreover, the detection of new buildings, which remains the most important part when updating maps, is complete (9/9); eventually, the detection of difficult configurations (typically new buildings built at the same location as destroyed ones) is possible with our algorithm (Figure 11-6).
In the present (and initial) state of the development of our method, fully automatic change detection is therefore not achieved yet. However, our method can already be considered as an efficient interactive tool to support change detection and updating, and also to reduce the time-consuming aspect of such a work.

5 CONCLUSION AND FUTURE WORK

Our goal was to build a system to detect changes in the building layer of a 2D cadastral database. The system described here show

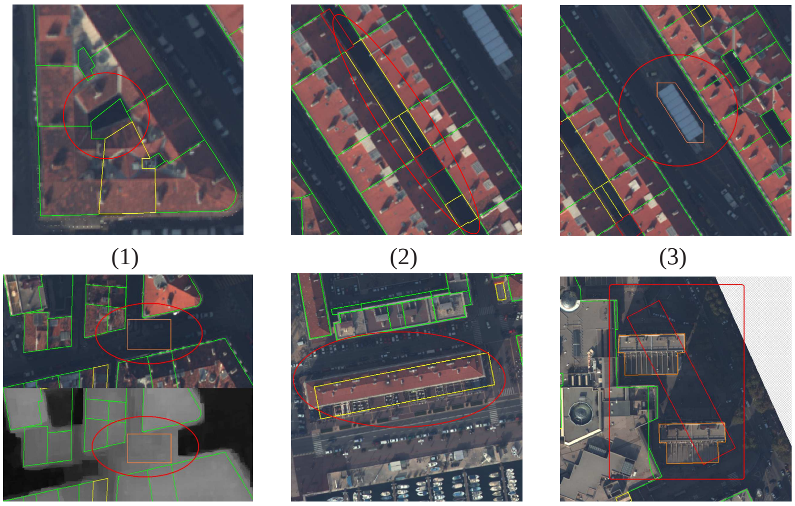

(1) (2) (3)

(4) (5) (6)

Figure 11: Evaluation Details. The colour code (Green / Yellow / Red / Orange) is the same as Figure 9. **(1) :** (FN) Inaccuracy in planimetry not detected. **(2) :** (FP) Internal structures. **(3) :** (FP) Building-like objects. **(4) :** (FP) Height inaccuracy in DSM. **(5) :** (TP) Inaccuracy in planimetry detected. **(6) :** (TP) Detection of destroyed and new buildings, even when located at the same place.

a very high potential, as all the factual changes (especially new buildings) in the study test area are detected, except for 2 minor changes. False alarms are almost caused either by building-like objects that do no need to be registered in the final up-to-date database (prefabs, footbridges . . .) or height inaccuracies in the initial DSM.

We plan to test our method in a more challenging context, typically with high-resolution satellite imagery. Here again, the detection of new buildings does not appear as the critical point of the method. Tests have already been carried out with Pleiades imagery, with a GSD of 70cm (Durupt et al., 2006) and show that the processed DTM is accurate enough to extract, after appropriate filtering processes, new buildings correctly. Future work will also focus on improving the performance of the first step of the method. For that purpose, a similarity measure, computed between contours extracted from aerial images and buildings, is being considered and should be added to our decision-making process: the main challenge here remains to assign the right height to the 2D building boundaries (from noisy correlation DSM).

REFERENCES

Busch, A., Gerke, M., Grünreich, D., Heipke, C., Liedtke, C. and Müller, S., 2004. Automated verification of a topographic reference dataset: System design and practical results. In: International Archives of Photogrammetry and remote Sensing, Vol. XXXV, Part B2, Istanbul, Turkey, pp. 735–740.

Champion, N. and Boldo, D., 2006. A robust algorithm for estimating Digital Terrain Models from Digital Surface Models in dense urban areas. In: ISPRS Commission 3 Symposium on Photogrammetric Computer Vision (PCV06), Bonn, Germany.

Deriche, R., 1987. Using Cannys criteria to derive a recursively implemented optimal edge detector. International Journal of Computer Vision.

Durupt, M., Flamanc, D., Le Bris, A., Iovan, C. and Champion, N., 2006. Evaluation of the potential of Pleiades system for 3D city models production: building, vegetation and DTM extraction. In: Proceedings of the ISPRS Commission I Symposium.

Fawcett, T., 2004. Roc graphs: Notes and practical considerations for researchers. Technical report, HP Laboratories, USA.

Förstner, W., 1994. Diagnotics and performance evaluation in computer vision. In: Performance versus Methodology in Computer Vision, NSF/ARPA Workshop, IEEE Computer Society.

Heipke, C., Mayer, H., Wiedemann, C. and Jamet, O., 1997. Evaluation of automatic road extraction. In: International Archives of Photogrammetry and Remote Sensing, Vol. XXXII, pp. 47–56.

Iovan, C., Boldo, D. and Cord, M., 2007. Automatic extraction of urban vegetation structures from high resolution imagery and Digital Elevation Model. In: Proceedings of 4th International Symposium Remote Sensing and Data Fusion over urban areas (URBAN 2007), Paris, France. To Appear.

Jordan, M., Cord, M. and Belli, T., 2002. Building detection from high resolution Digital Elevation Models in urban areas. In: International Archives of Photogrammetry and Remote Sensing, Vol. XXXIV, Part B3, Graz, Austria.

Matikainen, L., Hyyppä, J. and Kaartinen, H., 2004. Automatic detection of changes from laser scanner and aerial image data for updating building maps. In: International Archives of the Photogrammetry, Remote Sensing and Spatial Information Sciences, Istanbul, Turkey, pp. 434–439.

Müller, S. and Zaum, D. W., 2005. Robust building detection in aerial images. In: Proceedings of the ISPRS Workshop CMRT 2005, Vienna, Austria, pp. 143–148.

Olsen, B. and Knudsen, T., 2005. Automated change detection for validation and update of geodata. In: Proceedings of 6th Geomatic Week, Barcelone, Spain.

Pierrot-Deseilligny, M. and Paparoditis, N., 2006. An optimization-based surface reconstruction from Spot5-HRS stereo imagery. In: International Archives of Photogrammetry and Remote Sensing, Vol. XXXVI, Ankara, Turkey.

Rottensteiner, F., Trinder, J., Clode, S. and Kubik, K., 2005. Using the Dempster-Shafer method for the fusion of lidar data and multi-spectral images for building detection. Information Fusion pp. 283–300.

Steinnocher, K. and Kressler, F., 2006. Change detection. Technical report, EuroSDR Report.

Taillandier, F., 2005. Automatic building reconstruction from cadastral maps and aerial images. In: Proceedings of the ISPRS Workshop CMRT 2005, Vienna, Austria.

Tarsha-Kurdi, F., Landes, T., Grussenmeyer, P. and Smiegel, E., 2006. New approach for automatic detection of buildings in airborne laser scanner data using first echo only. In: ISPRS Commission 3 Symposium on Photogrammetric Computer Vision (PCV06), Bonn, Germany.